Struct Chem (2015) 26:859–871
DOI 10.1007/s11224-014-0552-x

ORIGINAL RESEARCH

Structural, electronic and reactivity studies on group 15 analogues of *N*-heterocyclic carbene

Manash Protim Borpuzari · Ankur Kanti Guha · Rahul Kar

Received: 30 July 2014 / Accepted: 15 December 2014 / Published online: 4 January 2015

Abstract The present article reports density functional studies on the Group 15 analogues of *N*-heterocyclic carbene (NHC) on their structure, reactivity, stability and ligating properties. Long-range corrected density functionals have been used due to its recent success in predicting orbital energies. These ligands are found to have greater π-accepting ability than NHC. Electron-donating substituents have a dramatic effect on their stability as well as ligating properties. Furthermore, natural resonance theory (NRT) calculations have been performed to determine the percentage weighting of resonance contributing structures. In addition, density-based global reactivity descriptors such as chemical potential, hardness, electrophilicity index and softness are calculated using four different density functional methods, and compared with CCSD(T) results. Moreover, the density-based local reactivity descriptors are employed to study the reactivity of Group 15 analogues. From the plot of dual descriptors, it is found that the "ene" centre of the Group 15 analogues of NHC is pseudodual.

Keywords Group 15 NHC · DFT · Stability · Ligating property · Reactivity descriptors · NBO

Electronic supplementary material The online version of this article (doi:10.1007/s11224-014-0552-x) contains supplementary material, which is available to authorized users.

M. P. Borpuzari · A. K. Guha · R. Kar (✉)
Department of Chemistry, Dibrugarh University, Dibrugarh 786004, Assam, India
e-mail: rahul.kar.dib@gmail.com

Introduction

Recently, the chemistry of stable metal-free singlet *N*-heterocyclic carbene (NHC) **1** (Scheme 1) has been of great interest [1–3]. The synthesis of numerous *N*-heterocyclic carbene has increased the opportunities for designing rational organometallic catalysts [2, 3]. Its flexibility has triggered many researchers to explore its ligation property and isolation. For instance, isolation of various main group derivatives of **1** has been achieved recently [4–17]. In principle, substitution of the carbenic carbon in **1** by Group 15 cation may resemble a similar bonding situation. Moreover, the presence of an extra positive charge at the "ene" centre in these Group 15 cations may influence their electronic properties to a great extent. As a result, their ligation properties (mainly σ donation/π acceptance) may be expected to be influenced greatly.

In one of the recent studies, Caputo et al. [14] reported the structural and reactivity studies of *N*-heterocyclic phosphenium (NHP) by energy decomposition analysis (EDA) of the M–P bond. Earlier, experimental and theoretical studies showed that stable nitrenium ions, like their carbene analogues, can exist [18]. Moreover, experimental and theoretical studies of neutral *N*-heterocyclic P-halophosphines revealed that the P–X bond can be considered as ionic bond [19–23]. Furthermore, studies on P-phospholyl-substituted *N*-heterocyclic phosphines indicated that this class of compound can be considered as a hybrid between phosphenium–phospholide donor–acceptor complexes and genuine covalent molecules [24]. On the other hand, on the basis of computational studies, it has been found that increasing formal replacement of CH units in the phosphole ring by phosphorus atoms causes a decrease in covalent bond order [25]. Very recently, DFT studies have shown that phosphines with *N*-heterocyclic boranyl

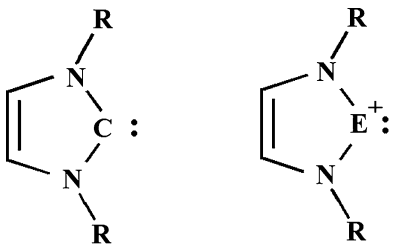

1 **E = N (2), P (3)**

R = H, Cl, Me, NH_2, OH, OMe, CN

Scheme 1 Schematic representation of NHC (**1**) and its group 15 (**2–3**) analogues

substituents lack a significant electrophilic character at boron, but may act as potential σ-donor/π-acceptor ligands through the phosphorus atom [26]. Another recent study on NHP revealed that binding of the first metal centre deactivates the opposite binding site and thus, strongly inhibits the formation of dinuclear complexes [27]. The extra stability attained by the transition metal complexes of NHC ligands over the phosphines is due to the superior σ-donation ability of the former, and for the Group 15 complexes, the stability is due to superior π-acceptor capability [28]. Quantum chemical calculation has also been performed to study the electronic structure of main group carbene analogues [29].

Recently, transition metal complexes of **2** and **3** have been structurally characterized where the ligands bind to the transition metals in a tridentate fashion [9–12]. Both experimental and theoretical studies reveal that these ligands have weaker σ-donation abilities but stronger π-accepting abilities [9–12]. Moreover, Choudhury has highlighted the chemistry of these Group 15 analogues of carbene [30]. The higher π acidity of these ligands may have wide implications in catalysis. Notably, Fürstner et al. have shown that the π-acceptor properties of NHCs may influence the outcome of gold-catalyzed reactions [31], thus, highlighting the importance of these π-acceptor ligands in catalysis. Furthermore, it has been found that *N*-heterocyclic phosphenium cations are isolobal analogues of nitrosyls [9], which implies that these Group 15 analogues of NHC may be suitable for promoting redox reaction at transition metal complexes. Additionally, non-innocent behaviour of *N*-heterocyclic phosphenium cation may be useful for its utilization in transition metal-based catalysis [10, 11]. Moreover, it has been observed that substituents attached to the N atoms of NHC have a dramatic effect on the structure, stability and reactivity of NHCs [32]. This has prompted us to undertake systematic quantum chemical calculations on the effect of substituents on the structure, reactivity, stability and ligating properties of **2** and **3** (Scheme 1). Although some theoretical studies on these Group 15 cations are there in the literature [9–12, 14–17, 29], to the best of our knowledge, no such studies were devoted towards understanding the effect of substituents on these Group 15 cations. In addition, wherever possible, comparison is made between these Group 15 cations with typical NHC (**1**). The rest of our paper is presented as follows: In "Theoretical and computational details" section, we present the theoretical and computational details employed in this paper. Structural, electronic, stability and reactivity of Group 15 analogues of NHCs are discussed in the results and discussion section. Lastly, in "Conclusions" section, we present our conclusions.

Theoretical and computational details

According to the first Hohenberg–Kohn theorem [33], the ground state energy of a system is a functional of electron density ρ and explicitly depends on external potential v. Derivative(s) of energy with respect to the number of electrons N defines the global reactivity descriptor (GRD) [34] such as chemical potential (μ) [35], hardness (η) [36] and softness (S) [37]. Operational definition of μ and η, using the finite difference approximation and Koopmans' theorem, [38, 39] are

$$\mu = \frac{-(\mathrm{IP} + \mathrm{EA})}{2}, \qquad \eta = \frac{(\mathrm{IP} - \mathrm{EA})}{2}$$

and $\mu = \frac{\varepsilon_{\mathrm{LUMO}} + \varepsilon_{\mathrm{HOMO}}}{2}$, and $\eta = \frac{\varepsilon_{\mathrm{LUMO}} - \varepsilon_{\mathrm{HOMO}}}{2}$ respectively.

On the other hand, local reactivity descriptors (LRD) are used in describing the local reactivity and selectivity of atoms in a molecule. Some important LRDs are local softness [37], condensed Fukui function (CFF) [40, 41] and dual descriptor ($\Delta f(r)$) [42]. Dual descriptors are found to be useful for studying ambiphilic molecule [43]. Moreover, electrophilicity of a ligand is measured by electrophilicity index (ω) [44] and its local part known as local philicity [45].

All the molecules are fully optimized without any symmetry constraint at B3LYP [46–48] level of theory with 6-311++G(d,p) [49, 50] basis set. The nature of stationary points has been characterized by frequency calculation at the same level of theory. All the structures have been found to be local minimum with real frequencies. Single-point energy calculations on the B3LYP-optimized geometries have been carried out for cation, anion and neutral Group 15 analogues of NHC with B3LYP, LC-BOP [51] ($\mu = 0.47$), CAM-B3LYP [52] and ωB97X-D [53] using 6-311++G(d,p) basis set. We calculated chemical potential, hardness, and electrophilicity index using both ΔSCF and orbital energies. However, CFF and dual descriptor were calculated using the Löwdin-based population for neutral and charged species. The hydrogenation energies are calculated by the energy difference between the cationic hydrogenated product and

the sum of energies of the cationic ligands and molecular hydrogen, and the carbene stabilization energy has been calculated using an isodesmic reaction (vide infra). All optimization and single-point energy calculations have been performed using GAMESS software [54]. Moreover, CCSD(T)/6-311++G(d,p) calculations on B3LYP-optimized geometries have been carried out for cation, anion and neutral molecules using ORCA suite of programme [55]. Dual descriptors are plotted using density difference method. Average local ionization energy has been calculated with contour value of 0.001 au. Natural bond orbital analysis is performed using NBO 6.0 [56] suite of programme.

Results and discussion

Molecular geometries

The optimized geometries of the parent molecules **2** and **3** (R=H) are shown in Fig. 1 and the others are shown in Supporting Information. The five-membered rings in all the molecules are perfectly planar. The geometrical parameters are compared with average experimental value for different substitution at *N*,*N* position with respect to "ene" centre and have been taken from reference [29] and collected in Table 1. We have obtained a reasonable agreement between the calculated and experimental [29] geometrical parameters. The angle at the central nitrogen atom (<NNN) of **2** is found to be obtuse whilst it is acute in case of **3**. This has also been observed by Tuononen et al. [29]. This might be due to the larger atomic radius of the central phosphorous atom in **3** compared to nitrogen atom in **2**. From Table 1, it can also be observed that <ENC and <NCC bond angle of **3** is slightly greater than that of **2**. The computed bond lengths in all the molecules are shorter than the respective single bonds, which suggest the delocalization of π electrons within the five-membered ring. This is in tune with previous study of Tuononen et al. [29] where these Group 15 analogues were predicted to gain aromatic stabilization like NHCs.

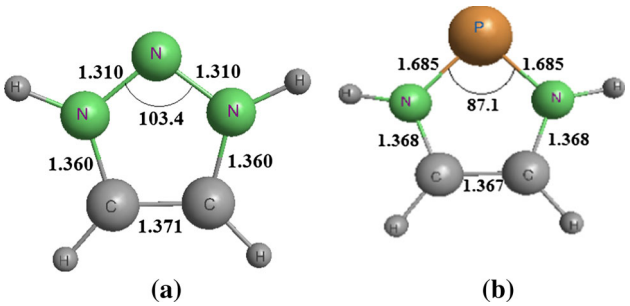

Fig. 1 Optimized geometries of the parent molecule, **a 2H** and **b 3H** at B3LYP/6-311++G(d,p). Bond lengths are in Å and angles are in degrees

The central E–N (E=N^+, P^+) bond length of **2** follows the order H < Me=Cl < CN=OH=NH_2=OMe whilst for **3**, the E–N bond length follows the order H < NH_2 < Cl < Me < CN=OH=OMe. Thus, all the substituents cause elongation of the E–N bond compared to the unsubstituted one, i.e. with hydrogen as the substituent. Furthermore, the C–N bond length of **2** follows the order OH < H=Me=NH_2=OMe < Cl < CN whereas for **3**, the C–N bond length follows the order OH=OMe < Me=Cl < H < NH_2 < CN. On the other hand, the C–C bond length with CN substituent is found to be lowest. It should be noted that no clear-cut trend of the variation of bond lengths in **2-3** as a function of substituents could be established.

Stability

The stability of these Group 15 analogues is of prime importance. Hence, we calculated their stabilities using the

Table 1 B3LYP/6-311++G(d,p) optimized and experimental geometrical parameters [29] for **2** and **3**

	Expt	H	Me	Cl	CN	OH	NH_2	OMe
2								
r(EN)	1.318	1.310	1.315	1.315	1.320	1.320	1.320	1.320
r(NC)	1.345	1.360	1.360	1.363	1.380	1.350	1.360	1.360
r(CC)	1.355	1.371	1.370	1.370	1.360	1.380	1.370	1.380
<NEN	103.8	103.4	105.1	102.9	103.1	102.3	103.7	102.7
<ENC	112.6	113.7	112.1	113.9	113.6	114.5	113.1	114.2
<NCC	105.6	104.5	105.2	104.6	104.9	104.4	105.0	104.5
3								
r(EN)	1.651	1.685	1.707	1.706	1.710	1.710	1.690	1.710
r(NC)	1.368	1.368	1.366	1.366	1.390	1.360	1.370	1.360
r(CC)	1.343	1.367	1.369	1.369	1.360	1.370	1.370	1.370
<NEN	90.1	87.2	86.0	86.0	86.6	85.2	87.2	85.6
<ENC	113.6	115.9	116.4	116.4	115.7	117.3	115.7	116.9
<NCC	111.3	110.5	110.5	110.5	111.0	110.1	110.7	110.3

Bond lengths are in Å and bond angles are in degrees

Table 2 Calculated hydrogenation energies (HE, kcal/mol) and carbene stabilization energy (CSE, kcal/mol)

Molecule	HE	CSE
2H	34.09	214.22
2Cl	15.52	195.65
2Me	42.35	222.48
2CN	16.93	197.07
2OH	25.17	205.30
2NH$_2$	24.27	204.41
2OMe	16.72	196.85
3H	24.07	98.75
3Cl	25.72	100.40
3Me	33.57	108.25
3CN	15.06	89.74
3OH	25.94	100.62
3NH$_2$	23.08	97.76
3OMe	28.29	102.96

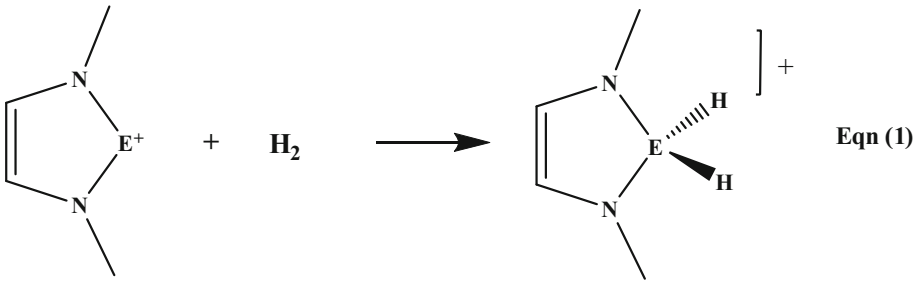

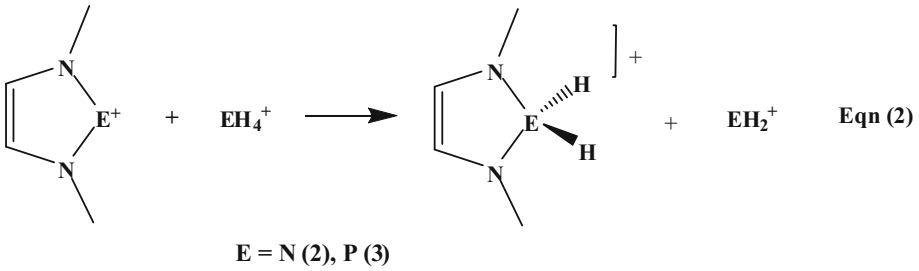

hydrogenation energy employing Eq. (1) in Table 2. The use of hydrogenation energy has been proposed as a measure of stability of carbenes [57]. In addition to the stability of these derivatives, the hydrogenation energies provide a clue to the hydrogen storage capacity [58] of carbenes. It should be noted that comparison of the hydrogenation energies for the neutral carbenes with these Group 15 cationic analogues will be erroneous as the values may be affected by different charge delocalization. However, comparison amongst a particular species (either carbenes or Group 15 cations) with varying substituents may be somewhat wiser.

The calculated hydrogenation energies are all positive (or the reaction (1) is endothermic) implying that the hydrogenated product is less stable than the separated reactants. Although the hydrogenated products have the ability to delocalize the charge over more number of atoms, it does not lead to higher stability of the products as revealed in Table 2. Rather, the cationic Group 15 NHC analogues are found to be more stable.

Barring few exceptions, hydrogenation energies for the electron-donating Me substituents are calculated to be the highest, whilst for electron-withdrawing substituents like Cl, CN etc., the calculated hydrogenation energies are lower. The higher endothermicity of the hydrogenation with electron-donating substituents may be due to the fact that electron-donating substituents may stabilize the positive charge at the "ene" centre, thereby rendering stability to the parent molecule. Somewhat higher endothermicity with substituents like OH, NH_2 and OMe may be due to the

Table 3 LC-BOP/6-311++G(d,p) calculated energies (in eV) of the σ-donating (E_σ), π-donating (E_π) and π-accepting (E_{π^*}) molecular orbitals

Molecule	E_σ	E_π	E_{π^*}
1H	−9.42	−9.55	2.61
2H	−19.29	−16.89	−4.43
2Cl	−19.56	−17.06	−4.71
2Me	−18.39	−16.11	−3.60
2CN	−20.73	−18.12	−6.67
2OH	−19.73	−17.01	−4.54
2NH$_2$	−19.02	−16.44	−4.24
2OMe	−19.29	−16.39	−3.95
3H	−18.29	−14.93	−5.16
3Cl	−18.75	−15.06	−5.58
3Me	−17.52	−14.29	−4.58
3CN	−19.95	−16.14	−7.07
3OH	−17.96	−14.99	−5.39
3NH$_2$	−17.93	−14.59	−4.84
3OMe	−18.18	−14.53	−4.93

positive resonance (+R) effect which may stabilize the positive charge at the "ene" centre of these cationic Group 15 NHC analogues.

We have also calculated the carbene stabilization energy (CSE) using an isodesmic reaction (Eq. 2 in Table 2). The stabilization energy so obtained has been found to vary linearly with the dimerization energy of carbenes [59]. The higher the endothermicity of the reaction, higher will be the stability of the parent system.

Both the hydrogenation energies as well as the stabilization energies obtained by Eq. (1) in Table 2 follow a similar order. Thus, both hydrogenation energies and stabilization energies reveal that electron-donating +I groups such as Me as well as +R groups such as OH, NH_2, OMe increases the stability of these parent Group 15 NHC analogues.

Ligation property

To address the ligation property of these ligands, we have calculated the energy of the σ-donating, π-donating and π-accepting molecular orbitals centred on the central atom ("ene" centre) of **2** and **3.** Since the five-membered rings of all the molecules under consideration have mirror plane, the shape of the frontier orbitals clearly reveals typical σ- and π-type characters. It has been known that the orbital energies cannot be accurately predicted from the conventional density functionals i.e. they depend on the form of the functional. However, recent studies suggest that the long-range-corrected (LC) density functionals could overcome this problem and could reproduce correct orbital energies [60]. Thus, in this article, we have employed LC functionals (LC-BOP, CAM-B3LYP and ωB97X-D) to compute the orbital energies and the LC-BOP values are presented in Table 3.

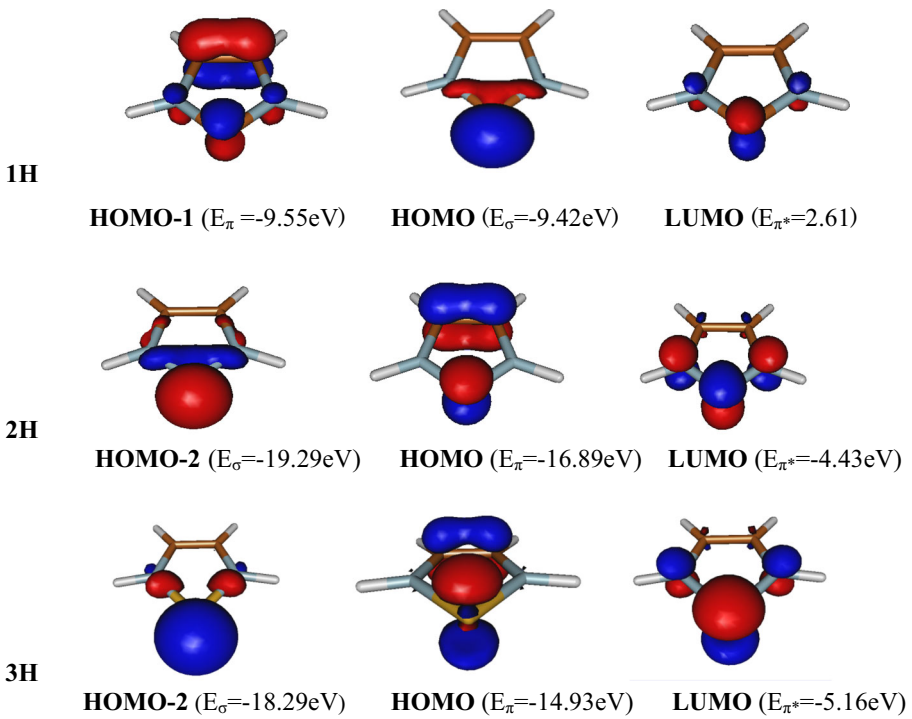

Fig. 2 Isosurface of Frontier MOs responsible for σ donation, π donation and π acceptance of **1H**, **2H** and **3H** computed at LC-BOP/6-311++G(d,p) with a contour value of 0.1

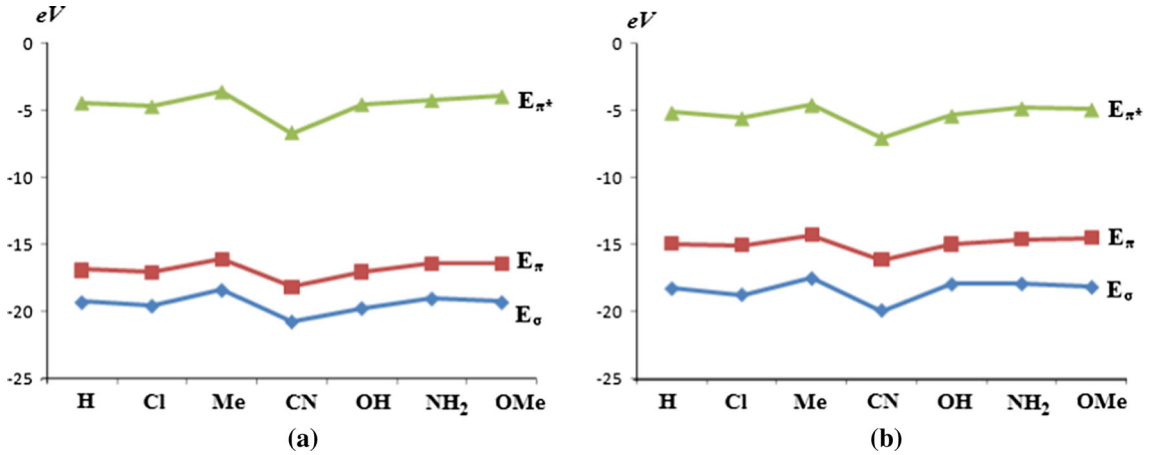

Fig. 3 Comparison of the σ- and π-donating and π-accepting ability of **a 2** and **b 3** as a function of different substituents

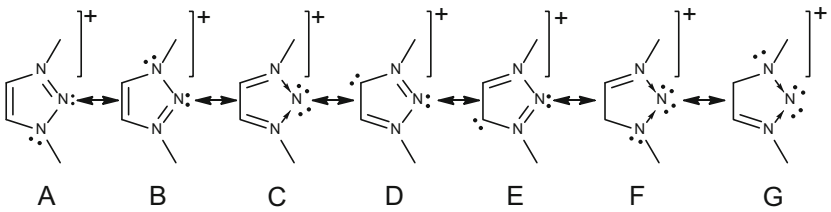

Fig. 4 NRT summary of **2** and **3** calculated at LC-BOP/6-311++G(d,p) level of theory

	% Weightage of A	% Weightage of B	% Weightage of C	% Weightage of D	% Weightage of E	% Weightage of F	% Weightage of G
2H	21.50	21.49	13.43	12.03	12.03	-	-
2Cl	19.31	19.31	12.02	11.11	11.11	-	-
2Me	19.85	19.77	13.06	11.81	11.81	-	-
2CN	19.84	19.84	8.70	9.77	9.77	-	-
2OH	17.30	17.23	13.23	11.41	11.37	3.79	3.79
2NH$_2$	18.76	18.75	12.97	11.30	11.27	3.72	3.72
2OMe	16.37	16.04	12.21	11.09	10.95	3.55	3.55
3H	23.97	23.97	9.57	12.88	12.87	-	-
3Cl	21.60	21.60	9.25	12.44	12.43	-	-
3Me	21.69	21.68	9.84	12.67	12.66	-	-
3CN	47.81	-	-	-	-	-	-
3OH	20.84	20.74	9.77	12.22	12.12	-	-
3NH$_2$	19.52	19.51	9.56	11.89	11.87	-	-

Group 15 analogues of NHCs have been predicted to have weaker σ-donation abilities and stronger π-accepting abilities compared to NHC [9–12, 28, 30], thus, we feel reasonable to compare the energies of the σ-donating and π-accepting orbitals of these Group cationic 15 analogues with parent NHC. This provides a quick comparison of the ligating properties of this class of compounds across a period as well as the effect of the extra positive charge at the ene centre of these Group 15 analogues. The frontier molecular orbitals of **1H**, **2H** and **3H** are shown in Fig. 2. Rest is available in the supporting information. It is evident from Fig. 2 and Table 3 that the σ-donation and π-donation abilities of these Group 15 analogues (**2** and **3**) are poor compared to NHC (**1**). For instance, the σ-donation (and π-donation) abilities of **1H**, **2H** and **3H** are −9.42 (−9.55), −19.29 (−16.89) and −18.29 (−14.93) eV, respectively. However, their π acceptance ability is strikingly better than **1**. This is evident from their orbital energies i.e. **1H**, **2H** and **3H** has π*energies of 2.61, −4.43, −5.16 eV, respectively (Table 3; Fig. 2). On the other

hand, the π-donation ability is found to be greater than σ donation ability for **2** and **3** (Table 3). It has also been observed that in case of NHC (**1**), the energy difference between σ and π donating orbitals is very small, whereas the difference is large in case of Group 15 analogues of NHC (**2**, **3**). These observations may reveal that in case of **1**, both σ and π orbitals contribute more or less equally towards bonding with metal fragment whereas in case of **2** and **3**, π orbitals contributes more towards bonding than σ orbital. It should be mentioned that both σ and π orbitals are more stabilized with LC functionals than that of B3LYP, whereas the reverse is found to be true in case of π*orbitals. Moreover, we observed that the HOMO in **1H** is of σ type whereas it is of π symmetric in **2H** and **3H**.

Table 3 reveals that the π-accepting ability of **3** is more than that of **2**. Table 3 and Fig. 3 also reveal electron-donating substituents like Me increases the σ- and π-donating ability of these ligands whilst electron-withdrawing substituents like CN decreases the same. However, the π-accepting ability of **2** and **3** dramatically increases with CN substituent. This observation has been pictorially represented in Fig. 3. The effect of substituents is found to be similar for both **2** and **3**.

Natural resonance theory (NRT) and natural bonding orbital (NBO) analyses

To investigate the nature of bonding, we performed natural resonance theory (NRT) analysis. NRT provides the description of total electron density in terms of a series of idealized resonance forms [61–63]. Each resonance form is given a weighting, which reflects the relative contribution of the resonance form to the total electron density. Figure 4 represents the contributing resonance forms of **2** and **3** (except 3OMe).

The resonance forms A and B have the major contribution, whilst the resonance form C has significant contribution (Fig. 4). It should also be noted that the resonance forms D and E have a comparable weight to resonance form C. In all these molecules, no single Lewis structure is adequate to describe the total electron density (except **3CN**). Moreover, in the cases of **2OH**, **2NH$_2$** and **2OMe**, NRT calculation predicted seven primary resonance structures (resonance structure A, B, C, D, E, F and G). The resonance forms C, F and G arise due to the donation of lone pairs from the adjacent N atoms to the "ene" centre, thereby rendering two lone pairs at the central E atom. It can be observed that, in case of **2**, resonance form C contributes more to the total electron density than that of resonance forms D and E (Fig. 4). On the other hand, for **3**, resonance forms D and E contribute more to the total electron density than that of C. It is worthy to note that the reactivity of the germylene and stannylene analogues is in accordance with a contribution of resonance structure C [64]. This resonance form may be identical to that of recently developed chemistry of element (0) [65–70]. Recently, Bharatam et al. have highlighted the chemistry of divalent N(I) compounds which possess two lone pairs [70]. The resonance form C is also identical to that of N(I) compound with two lone pairs. Moreover, the contribution of this resonance form is significant which implies that these compounds may also act as double Lewis bases owing to the presence of two lone pairs. Thus, the NRT results indicate that these Group 15 cationic analogues of carbenes may resemble similar reactivities as that of the heavier analogues of carbene as well as that of element(0) compounds [64–70].

The natural bond orbital (NBO) analysis provides a valence-bond-type description of a molecule by providing a single best Lewis-like depiction of the total electron density. Thus, we have performed the NBO analysis of these ligands to better understand the bonding situation. We present the hybridization of the lone pair (LP), electron occupancy, natural charge (q_E) and occupancy of the out-of-plane p orbital (p_π) at the "ene" centre (Table 4). The hybridization of the "ene" centre is almost sp for **2**, whilst the s character increases when the central E atom is changed from N to P (as in **3**). The occupancy of the lone pair is close to 2.00 e which implies that the lone pair is almost localized at the "ene" centre. The natural charges at the "ene" are more positive for **3** compared to **2**. This indicates that **3** is more electrophilic than **2**. This is in accordance with the calculated energies of the π-accepting orbitals (E_{π^*}) which are found to be lower for **3** than **2**.

Table 4 NBO analysis of 2 and 3 at B3LYP/6-311++G(d,p) level of theory

Molecule	Hybridization of the LP	Occupancy	q_E	p_π
2H	$sp^{1.03}$	1.95	0.05	1.13
2Cl	$sp^{1.00}$	1.95	0.04	1.48
2Me	$sp^{1.07}$	1.95	0.02	1.43
2CN	$sp^{0.93}$	1.96	0.10	1.13
2OH	$sp^{0.95}$	1.95	−0.02	1.22
2NH$_2$	$sp^{0.99}$	1.95	0.00	1.17
2OMe	$sp^{0.98}$	1.94	−0.02	1.41
3H	$sp^{0.30}$	1.98	1.13	0.89
3Cl	$sp^{0.26}$	1.98	1.16	0.93
3Me	$sp^{0.31}$	1.98	1.09	0.94
3CN	$sp^{0.25}$	1.99	1.24	0.86
3OH	$sp^{0.26}$	1.98	1.10	0.95
3NH$_2$	$sp^{0.28}$	1.98	1.18	0.87
3OMe	$sp^{0.27}$	1.98	1.08	0.92

Table 5 DFT-based global reactivity descriptors using orbital energies

	2H	2Cl	2Me	2CN	2OH	$2NH_2$	2OMe	3H	3Cl	3Me	3CN	3OH	$3NH_2$	3OMe
μ														
CCSD(T)	−0.38	−0.38	−0.35	−0.44	−0.38	−0.37	−0.36	−0.36	−0.36	−0.33	−0.41	−0.36	−0.34	−0.34
B3LYP	−0.39	−0.39	−0.35	−0.43	−0.38	−0.36	−0.35	−0.36	−0.37	−0.34	−0.41	−0.36	−0.35	−0.35
LC-BOP	−0.39	−0.39	−0.36	−0.45	−0.40	−0.38	−0.37	−0.37	−0.38	−0.35	−0.43	−0.37	−0.36	−0.36
CAM-B3LYP	−0.39	−0.39	−0.36	−0.44	−0.39	−0.38	−0.36	−0.37	−0.38	−0.34	−0.42	−0.37	−0.35	−0.35
ωB97X-D	−0.39	−0.39	−0.36	−0.44	−0.39	−0.37	−0.36	−0.37	−0.37	−0.34	−0.42	−0.37	−0.35	−0.35
η														
CCSD(T)	0.22	0.20	0.21	0.20	0.22	0.21	0.21	0.18	0.16	0.17	0.16	0.17	0.17	0.17
B3LYP	0.12	0.11	0.13	0.10	0.12	0.11	0.11	0.09	0.08	0.09	0.08	0.09	0.09	0.09
LC-BOP	0.23	0.22	0.23	0.20	0.23	0.22	0.22	0.18	0.17	0.18	0.17	0.18	0.18	0.18
CAM-B3LYP	0.18	0.17	0.18	0.15	0.18	0.17	0.17	0.14	0.13	0.13	0.12	0.13	0.14	0.13
ωB97X-D	0.20	0.19	0.20	0.17	0.20	0.19	0.19	0.16	0.15	0.16	0.15	0.16	0.16	0.16
S														
CCSD(T)	2.24	2.44	2.33	2.53	2.29	2.37	2.37	2.82	3.05	2.95	3.17	2.94	2.93	3.01
B3LYP	4.06	4.57	3.99	5.02	4.11	4.42	4.41	5.71	5.98	5.71	6.53	5.85	5.71	5.82
LC-BOP	2.18	2.26	2.18	2.46	2.18	2.23	2.27	2.78	2.87	2.80	3.00	2.84	2.79	2.83
CAM-B3LYP	2.82	2.99	2.79	3.29	2.83	2.92	2.98	3.69	3.82	3.71	4.06	3.77	3.70	3.76
ωB97X-D	2.51	2.67	2.49	2.90	2.52	2.60	2.64	3.16	3.26	3.18	3.44	3.22	3.17	3.21
ω														
CCSD(T)	0.32	0.35	0.29	0.48	0.33	0.32	0.30	0.36	0.40	0.33	0.53	0.38	0.35	0.35
B3LYP	0.60	0.68	0.50	0.94	0.60	0.59	0.54	0.75	0.81	0.65	1.12	0.78	0.69	0.70
LC-BOP	0.34	0.35	0.29	0.50	0.34	0.32	0.30	0.38	0.41	0.34	0.55	0.40	0.36	0.36
CAM-B3LYP	0.43	0.45	0.36	0.64	0.43	0.41	0.39	0.50	0.54	0.44	0.72	0.52	0.47	0.47
ωB97X-D	0.38	0.40	0.32	0.56	0.38	0.36	0.33	0.42	0.46	0.37	0.61	0.44	0.40	0.40

CCSD(T) values are calculated using finite difference approximation. Values are in a.u

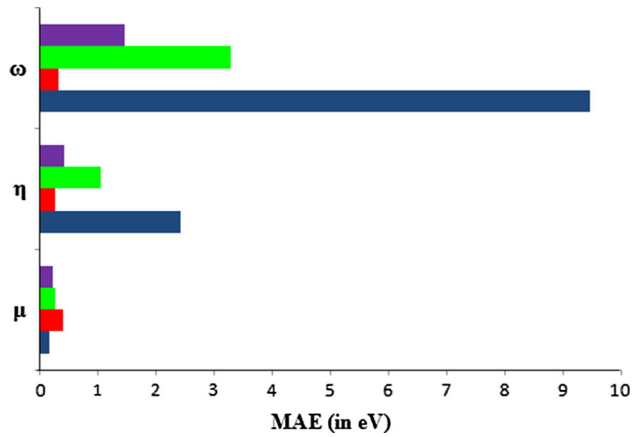

Fig. 5 Plot of mean absolute error (MAE) values (eV) for different functionals. *Blue colour* (B3LYP), *red colour* (LC-BOP), *green colour* (CAM-B3LYP) and *violet colour* (ωB97x-D) (Color figure online)

Reactivity descriptors

The DFT-based global and local reactivity descriptors such as chemical potential, hardness, softness, electrophilicity index, Fukui function, dual descriptor, local softness and local philicity are computed using both ΔSCF and Koopmans' theorem with four different functions. The reliability of these descriptors in understanding several chemical and biological systems has been tested extensively [71–73]. These reactivity descriptors have been used to describe the hard–soft acid–base interactions of silylenes and germylenes [74] and the effect of substituents on the properties of silylenes [75, 76] and carbenes [77].

In Table 5, we present the values of chemical potential, hardness, softness and electrophilicity index calculated using orbital energies and compare with CCSD(T) values (calculated from energies of neutral and charged species). It can be observed from the mean absolute error that LC functionals predict global reactivity descriptors more accurately than B3LYP (Fig. 5). In general, the better performance of LC functional is due to the fact that the LC functionals satisfy Koopmans' theorem [78], and hence, orbital energies computed with LC functional would be a good choice to calculate GRD. It should be noted that similar trends are observed with LC-BOP, CAM-B3LYP and ωB97x-D functional, and the LC-BOP results are discussed below.

Almost a constant chemical potential value is observed for all substitution of **2** and **3,** except **2CN** and **3CN**

Table 6 DFT-based local reactivity descriptors

	2H	2Cl	2Me	2CN	2OH	$2NH_2$	2OMe	3H	3Cl	3Me	3CN	3OH	$3NH_2$	3OMe
f_E^+														
B3LYP	0.24	0.26	0.19	0.17	0.19	0.19	0.18	0.38	0.32	0.33	0.30	0.35	0.35	0.33
LC-BOP	0.24	0.20	0.20	0.19	0.20	0.20	0.19	0.38	0.33	0.33	0.32	0.35	0.36	0.33
CAM-B3LYP	0.24	0.20	0.20	0.18	0.20	0.20	0.19	0.38	0.32	0.33	0.31	0.35	0.35	0.33
ωB97X-D	0.24	0.20	0.20	0.18	0.20	0.10	0.19	0.38	0.32	0.33	0.31	0.35	0.35	0.33
f_E^-														
B3LYP	0.30	−0.07	0.21	0.03	0.05	0.07	0.03	0.34	0.30	0.32	0.27	0.33	0.31	0.30
LC-BOP	0.30	0.03	0.21	0.20	0.23	0.04	0.03	0.31	0.30	0.31	0.29	0.34	0.30	0.31
CAM-B3LYP	0.30	0.03	0.21	0.03	0.05	0.14	0.03	0.32	0.30	0.31	0.28	0.33	0.31	0.31
ωB97X-D	0.31	0.03	0.21	0.03	0.05	0.05	0.03	0.32	0.30	0.32	0.29	0.33	0.31	0.31
s_E^+														
B3LYP	0.96	1.17	0.76	0.87	0.80	0.85	0.81	2.19	1.92	1.87	1.98	2.02	1.98	1.90
LC-BOP	0.53	0.45	0.44	0.46	0.44	0.45	0.44	1.07	0.93	0.93	0.97	0.98	1.00	0.94
CAM-B3LYP	0.67	0.58	0.55	0.59	0.56	0.57	0.56	1.41	1.23	1.22	1.26	1.30	1.30	1.23
ωB97X-D	0.60	0.53	0.50	0.52	0.51	0.26	0.50	1.21	1.05	1.05	1.07	1.12	1.11	1.05
s_E^-														
B3LYP	1.23	−0.30	0.83	0.17	0.22	0.31	0.14	1.94	1.80	1.81	1.79	1.94	1.79	1.76
LC-BOP	0.67	0.06	0.46	0.50	0.50	0.08	0.06	0.87	0.85	0.86	0.88	0.97	0.85	0.87
CAM-B3LYP	0.86	0.10	0.58	0.09	0.14	0.40	0.09	1.18	1.15	1.16	1.16	1.23	1.14	1.16
ωB97X-D	0.77	0.09	0.52	0.08	0.13	0.14	0.08	1.03	0.99	1.01	0.98	1.06	0.99	1.00
ω_E^+														
B3LYP	0.14	0.17	0.10	0.16	0.12	0.11	0.10	0.29	0.26	0.21	0.34	0.27	0.24	0.23
LC-BOP	0.08	0.07	0.06	0.09	0.07	0.07	0.06	0.15	0.13	0.11	0.18	0.14	0.13	0.12
CAM-B3LYP	0.10	0.09	0.07	0.11	0.09	0.08	0.07	0.19	0.17	0.14	0.22	0.18	0.16	0.15
ωB97X-D	0.09	0.08	0.06	0.10	0.08	0.04	0.06	0.16	0.15	0.12	0.19	0.15	0.14	0.13
ω_E^-														
B3LYP	0.18	−0.04	0.10	0.03	0.03	0.04	0.02	0.25	0.24	0.21	0.31	0.26	0.22	0.21
LC-BOP	0.10	0.01	0.06	0.10	0.08	0.01	0.01	0.12	0.12	0.10	0.16	0.14	0.11	0.11
CAM-B3LYP	0.13	0.01	0.08	0.02	0.02	0.06	0.01	0.16	0.16	0.14	0.21	0.17	0.14	0.15
ωB97X-D	0.12	0.01	0.07	0.01	0.02	0.02	0.01	0.14	0.14	0.12	0.17	0.14	0.12	0.12
Δf_E														
B3LYP	−0.07	0.32	−0.02	0.14	0.14	0.12	0.15	0.04	0.02	0.01	0.03	0.01	0.03	0.02
LC-BOP	−0.06	0.17	−0.01	−0.02	−0.03	0.17	0.17	0.07	0.03	0.03	0.03	0.00	0.05	0.02
CAM-B3LYP	−0.07	0.16	−0.01	0.15	0.15	0.06	0.16	0.06	0.02	0.02	0.03	0.02	0.04	0.02
ωB97X-D	−0.07	0.17	−0.01	0.15	0.15	0.05	0.16	0.06	0.02	0.01	0.02	0.02	0.04	0.02

Values are in a.u

(Table 5). Since CN has both -I and -R effect, so the escaping tendency of electron from **2CN** and **3CN** is lower than the other substitution. An inspection of hardness and softness values indicate that **2** is slightly harder than **3**. For instance, the chemical hardness value of **2H** and **3H** are 0.23 a.u. and 0.18 a.u., respectively (whereas softness values are 2.18 $a.u.^{-1}$ and 2.87 $a.u.^{-1}$, respectively). Moreover, in case of **2**, hardness of **2CN** is found to be lowest (0.20 a.u) (whereas softness of **2CN** is found to be highest (2.46 $a.u.^{-1}$)). On the other hand, in case of **3**, chemical hardness is almost constant, (whereas softness of **3CN** is highest (3.00 $a.u.^{-1}$)). It is evident from the inspection of electrophilicity index (Table 5) that **3** is slightly more electrophilic in nature. For instance, electrophilicity index of **2H** and **3H** are 0.34 and 0.38 a.u., respectively. Moreover, in case of **2**, electrophilicity index follows the order **2CN** > **2Cl** ≈ **2H** ≈ **2OH** > $\mathbf{2NH_2}$ > **2OMe** > **2Me** and in case of **3**, the order is **3CN** > **3Cl** ≈ **3OH** > **3H** > $\mathbf{3NH_2}$ ≈ **3OMe** > **3Me**.

In order to understand the reactivity of the "ene" centre, we employ the concepts of LRD, such as CFF and local softness. It can be observed from Table 6 that the f_E^+ value

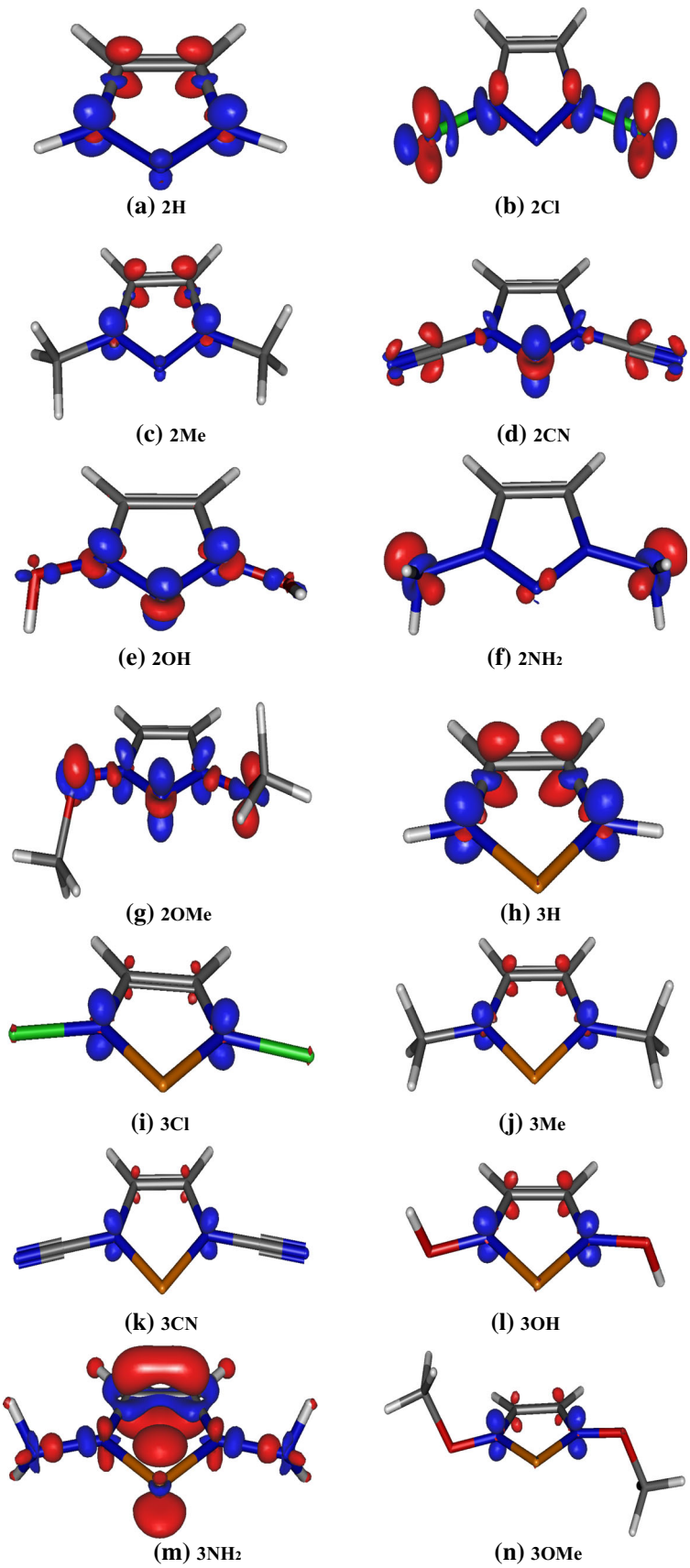

Fig. 6 Dual descriptor of **a 2H**, **b 2Cl**, **c 2Me**, **d 2CN**, **e 2OH**, **f 2NH$_2$**, **g 2OMe**, **h 3H**, **i 3Cl**, **j 3Me**, **k 3CN**, **l 3OH**, **m 3NH$_2$** and **n 3OMe** computed at B3LYP/6-311++G(d,p). *Blue-coloured region* indicates $\Delta f = 0.01$ au and *red-coloured surface* indicates $\Delta f = -0.01$ a.u (Color figure online)

Table 7 Magnitude and location $\bar{I}s_{,min}$ at B3LYP/6-311++G(d,p) basis set

Molecule	$\bar{I}s_{,min}$	Location
2H	15.44	C=C bond
2Cl	16.11	near Cl atom
2Me	14.59	C=C bond
2CN	15.92	near N atom of CN
2OH	15.57	C=C bond
2NH$_2$	13.64	near N atom of NH_2
2OMe	14.96	C=C bond
3H	14.13	near P atom
3Cl	14.03	near P atom
3Me	14.59	C=C bond
3CN	15.30	near P atom
3OH	13.98	near P atom
3NH$_2$	13.03	near N atom of NH_2
3OMe	13.48	near P atom

Values are in eV

for **3** is higher than **2**, which indicates that nucleophilic attack on the "ene" centre of **3** is more favourable. Moreover, f_E^+ decreases with substitutions. On the other hand, the variation of f_E^- value with substitution is different for **2** and **3**. For instance, f_E^- values of **2H**, **2Cl**, **2Me**, **2CN**, **2OH**, **2NH$_2$** and **2OMe** are 0.30, 0.03, 0.21, 0.20, 0.23, 0.04 and 0.03, respectively, whereas the corresponding values for **3** are 0.31, 0.30, 0.31, 0.29, 0.34, 0.30 and 0.31, respectively. These data clearly suggest that electrophilic attack on the "ene" centre of **2Cl**, **2NH$_2$** and **2OMe** are less favourable. The same trend is observed for s_E^+ and s_E^- also. An inspection of the ω_E^+ indicates that the "ene" centre of **3** is more electrophilic than that of **2** (Table 6). Moreover, the philicity of "ene" centre is highest for CN substitution in both **2** and **3**. On the other hand, the nucleophilicity of the "ene" centre of **3** (ω_E^- for **3H** is 0.12 a.u.) is slightly higher than **2** (ω_E^- for **2H** is 0.10 a.u.). However, ω_E^- for **2Cl**, **2NH$_2$** and **2OMe** is almost equal to zero i.e. 0.01 a.u. which indicates the absence of nucleophilic character at the "ene" centre. Interestingly, negative values of dual descriptor (Δf_E) are obtained for **2H**, **2Me**, **2CN** and **2OH** (Table 6) whilst slightly positive values are obtained for all NHPs, **3**. This small negative and positive value of dual descriptor infers the presence of ambiphilic nature at the "ene" centre. On the other hand, Δf_E value for **2Cl**, **2NH$_2$** and **2OMe** is 0.17 (Table 6) which indicates that the "ene" centre for these three molecules are favourable for nucleophilic attack. In order to get a better idea on the ambiphilic nature of the "ene" centre, we have plotted dual descriptor for these compounds. Dual descriptor plots of **2** and **3** are given in Fig. 6. In case of **2H** and **2Me**, positive lobe is observed at "ene" centre and negative lobe is present in the backbone of the ring. Thus, it may be concluded, on the basis of pseudodual behaviour of the "ene" centre, that it may donate electron from the heterocyclic ring through the "ene" centre. On the other hand, in case of **2CN**, **2OH** and **2OMe**, both positive and negative lobes are observed at the "ene" centre which indicates that in these molecules the "ene" centre shows genuine dual reactivity.

Average local ionization potential

The average local ionization energy $\bar{I}(r)$ [79, 80] is the energy necessary to remove an electron from the point r in the space of a system. Its lowest values reveal the locations of the least tightly held electrons, and thus the favoured sites for reaction with electrophiles or radicals. Moreover, average local ionization energy is usually computed on the surface of the molecule and it is denoted by $\bar{I}s(r)$. The points on the surface of the molecule with lowest $\bar{I}s(r)$ value ($\bar{I}s_{,min}$) is of particular interest and is widely used for prediction of sites for electrophilic or radical attack [81, 82]. Location and magnitude of $\bar{I}s_{,min}$ are presented in Table 7. In case of **2H**, **2Me**, **2OH**, **2OMe and 3Me**, $\bar{I}s_{,min}$ is found to be located near C=C bond which indicates that the C=C bond of these molecule is susceptible for electrophilic attack (Table 7). On the other hand, in case of **3H**, **3Cl**, **3CN**, **3OH** and **3OMe**, $\bar{I}s_{,min}$ is found to be located near the "ene" centre. Amongst all the substituents, **2Cl** (in case of **2**) and **3CN** (in case of **3**) have the highest $\bar{I}s_{,min}$ value which indicates that they have the lowest reactivity towards electrophilic attack.

Conclusions

In conclusion, we have calculated the stability, ligating property and reactivity of the Group 15 analogues of NHC using the density functional theory. The calculated hydrogenation and stabilization energies of these ligands are both endothermic which indicates their stability. Electron-donating +I substituents like Me and +R substituents like OH, NH_2, OMe increases the stability of these ligands by stabilizing the positive charge at the "ene" centre. These ligands possess superior π acidity than that of NHCs however, their σ basicity is lower. The presence of an extra positive charge in these Group 15 cationic analogues dramatically increases the π acidity of these ligands. Substituents have a dramatic effect on the ligating properties of these ligands. The higher π acidity of these ligands may help in stabilizing electron-rich metal centres, thereby rendering the metal centre more electrophilic character which may help during catalysis. In addition, NRT calculation was performed to study the resonance contributing

structures. It was found that these Group 15 analogues may resemble similar reactivities as that of the heavier analogues of carbene as well as that of element(0) compound. Furthermore, density-based global reactivity descriptors have been calculated using LC functionals and comparison with CCSD(T) values conclude that GRD may be accurately calculated with orbital energies. Moreover, on the basis of DFT-based local reactivity descriptor study, it can be concluded that the "ene" centre of Group 15 analogue of *N*-heterocyclic carbene is ambiphilic in nature and plot of dual descriptor indicated the pseuodual behaviour of "ene" centre.

Acknowledgments This work is dedicated to Dr. Sourav Pal on his 60th birthday. M. P. B thanks Council of Industrial and Scientific Research (CSIR), New Delhi, for financial assistance. RK thanks the SERB, Department of Science and Technology (DST), New Delhi for financial support [SB/FT/CS-132/2013]. The authors thank Netrakamal Bora for providing the optimized geometries for **2** and **3** with substituents **CN, OH, NH_2 and OMe** only.

References

1. Arduengo AJ III, Harlow RL, Kline M (1991) J Am Chem Soc 113:361–363
2. Melaimi M, Soleilhavoup M, Bertrand G (2010) Angew Chem Int Ed 49:8810–8849
3. Hahn FE, Jahnke MC (2008) Angew Chem Int Ed 47:3122–3172
4. Segawa Y, Yamashita M, Nozaki K (2006) Science 314:113–115
5. Segawa Y, Yamashita M, Nozaki K (2009) J Am Chem Soc 131:9201–9203
6. Schmidt ES, Jockisch A, Schmidbaur H (1999) J Am Chem Soc 121:9758–9759
7. Yoo H, Carroll PJ, Berry DH (2006) J Am Chem Soc 128:6038–6039
8. Herrmann WA, Denk M, Behm J, Scherer W, Klingan FR, Bock H, Solouki B (1992) Wagner. Angew Chem Int Ed Engl 31:1485–1488
9. Pan B, Xu Z, Bezpalko MW, Foxman BM, Thomas CM (2012) Inorg Chem 51:4170–4179
10. Day GS, Pan B, Kellenberger DL, Foxman BM, Thomas CM (2011) Chem Commun 47:3634–3636
11. Heims F, Pfaff FF, Abram SLL, Farquhar ER, Bruschi M, Greco C, Ray K (2014) J Am Chem Soc 136:582–585
12. Tulchinsky Y, Iron MA, Botoshansky M, Gandelman M (2011) Nat Chem 3:525–531
13. Carmalt CJ, Lomeli V, McBurnett BG, Cowley AH (1997) Chem Commun 21:2095–2096
14. Caputo CA, Jennings MC, Tuononen HM, Jones ND (2009) Organometallics 28:990–1000
15. Denk MK, Gupta S, Ramachandran R (1996) Tetrahedron Lett 37:9025–9028
16. Burck S, Daniels J, Gans-Eichler T, Gudat D, Nättinen K, Nieger M (2005) Z Anorg Allg Chem 631:1403–1412
17. Denk MK, Gupta S, Lough AJ (1999) Eur J Inorg Chem 1999:41–49
18. Boche G, Andrews P, Harms K, Marsch M, Rangappa KS, Schimeczek M, Willeke C (1996) J Am Chem Soc 118:4925–4930
19. Gudat D, Haghverdi A, Hupfer H, Nieger M (2000) Chem Eur J 6:3414–3425
20. Burck S, Gudat D, Nieger M, Benkö Z, Nyulászi L, Szieberth D (2009) Z Allg Anorg Chem 635:245–252
21. Gudat D (2010) Acc Chem Res 43:1307–1316
22. Gudat D, Haghverdi A, Nieger M (2000) Angew Chem Int Ed 39:3084–3086
23. Schmid D, Loscher S, Gudat D, Bubrin D, Hartenbach I, Schleid T, Benkö Z, Nyulászi L (2009) Chem Commun 2009:830–832
24. Burck S, Götz K, Kaupp M, Nieger M, Weber J (2009) Schmedt auf der Günne J, Gudat. J Am Chem Soc 131:10763–10774
25. Benkö Z, Burck S, Gudat D, Hofmann M, Lissner F, Nyulászi L, Zenneck U (2010) Chem Eur J 16:2857–2865
26. Gudat D, Kaaz M, Bender J, Förster D, Frey W, Nieger M (2013) Dalton Trans 43:680–689
27. Mourgas G, Nieger M, Förster D, Gudat D (2013) Inorg Chem 52:4104–4122
28. Wilson DJD, Couchman SA, Dutton JL (2012) Inorg Chem 51:7657–7668
29. Tuononen MH, Roesler R, Dutton JL, Ragogna PJ (2007) Inorg Chem 46:10693–10706
30. Choudhury J (2011) Angew Chem Int Ed 50:10772–10774
31. Alcarazo M, Stork T, Anoop A, Thiel W, Fürstner A (2010) Angew Chem Int Ed 49:2542–2546
32. Guha AK, Sarmah S, Phukan AK (2010) Dalton Trans 39:7374–7383
33. Hohenberg P, Kohn W (1964) Phys Rev 136:864–871
34. Parr RG, Yang W (1989) Density functional theory for atoms and molecules. Oxford University Press, New York
35. Parr RG, Donnelly RA, Levy M, Palke WE (1978) J Chem Phys 68:3801–3807
36. Parr RG, Pearson RG (1983) J Am Chem Soc 105:7512–7516
37. Yang W, Parr RG (1985) Proc Natl Acad Sci USA 82:6723–8726
38. Koopmans TA (1933) Physica 104:1–6
39. Szabo A, Ostlund NS (1996) Modern quantum chemistry introduction to advanced electronic structure theory. Dover Publication, Inc, Mineola, New York
40. Parr RG, Yang W (1984) J Am Chem Soc 106:4049–4050
41. Yang W, Mortier WJ (1986) J Am Chem Soc 108:5708–5711
42. Morell C, Grand A, Toro-Labbé A (2005) J Phys Chem A 109:205–212
43. Cárdenas C, Rabi N, Ayers PW, Morell C, Jaramillo P, Fuentealba P (2009) J Phys Chem A 113:8660–8667
44. Parr RG, Szentpaly LV, Liu S (1999) J Am Chem Soc 121:1922–1924
45. Chattaraj PK, Maiti B, Sarkar U (2003) J Phys Chem A 107:4973–4975
46. Becke AD (1993) J Chem Phys 98:5648–5652
47. Becke AD (1988) Phys Rev A 38:3098–3100
48. Lee C, Yang W, Parr RG (1988) Phys Rev B 37:785–789
49. Krishnan R, Binkley JS, Seeger R, Pople JA (1980) J Chem Phys 72:650–654
50. McLean AD, Chandler GS (1980) J Chem Phys 72:5639–5648
51. Iikura H, Tsuneda T, Yanai T, Hirao K (2001) J Chem Phys 115:3540–3544
52. Yanai T, Tew DP, Handy NC (2004) Chem Phys Lett 393:51–57
53. Chai JD, Gordon MH (2008) Phys Chem Chem Phys 10:6615–6620
54. Schmidt MW, Baldridge KK, Boatz JA, Elbert ST, Gordon MS, Jensen JH, Koseki S, Matsunga N, Nguyen KA, Su SJ, Windus TL, Dupuis M, Montgomery JA (1993) J Comput Chem 14:1347–1363
55. Neese F (2008) ORCA-An ab initio, Density functional and semiempirical program package, version 3.0–35, University of Bonn, Bonn

56. Glendening ED, Badenhoop JK, Reed AE, Carpenter JE, Bohmann JA, Morales CM, Landis CR, Weinhold F (2013) NBO 6.0, Theoretical chemistry Institute, University of Wisconsin, Madison
57. Dixon DA, Arduengo AJ III (2006) J Phys Chem A 110:1968–1974
58. Dixon DA, Gutowski M (2005) J Phys Chem A 109:5129–5135
59. Nyulászi L, Veszprémi T, Forró A (2000) Phys Chem Chem Phys 2:3127–3129
60. Kar R, Song JW, Hirao K (2013) J Comp Chem 34:958–964
61. Glendening ED, Weinhold F (1998) J Comput Chem 19:593–609
62. Glendening ED, Weinhold F (1998) J Comput Chem 19:610–627
63. Glendening ED, Badenhoop JK, Weinhold F (1998) J Comput Chem 19:628–646
64. Eichler TG, Gudat D, Nättinen K, Neiger M (2006) Chem Eur J 12:1162–1173
65. Petz W, Kutschera C, Heitbaum M, Frenking G, Tonner R, Neumüller B (2005) Inorg Chem 44:1263–1274
66. Tonner R, Frenking G (2008) Chem Eur J 14:3260–3272
67. Tonner R, Frenking G (2008) Chem Eur J 14:3273–3289
68. Tonner R, Frenking G (2009) Organometallics 28:3901–3905
69. Tonner R, Frenking G (2009) Pure Appl Chem 81:597–614
70. Patel DS, Bharatam PV (2009) Chem Commun 2009:1064–1066
71. Geerlings P, Proft FD, Langenaeker W (2003) Chem Rev 103:1793–1874
72. Chattaraj PK, Sarkar U, Roy DR (2006) Chem Rev 106:2065–2091
73. Geerlings P, Proft FD (2008) Phys Chem Chem Phys 10:3028–3042
74. Oláh J, Proft FD, Veszprémi T, Geerlings P (2005) J Phys Chem A 109:1608–1615
75. Oláh J, Veszprémi T, Proft FD, Geerlings P (2007) J Phys Chem A 111:10815–10823
76. Correa JV, Jaque P, Oláh J, Labbé AT, Geerlings P (2009) Chem Phys Lett 470:180–186
77. Kelemen Z, Hollóczki O, Oláh J, Nyulászi L (2013) RSC Adv 3:7970–7978
78. Tsuneda T, Song JW, Suzuki S, Hirao K (2010) J Chem Phys 133:174101–174109
79. Sjoberg P, Murray JS, Brink T, Politzer P (1990) Can J Chem 68:1440–1443
80. Politzer P, Murray JS, Bulat FA (2010) J Mol Model 16:1731–1742
81. Bulat FA, Burgess JS, Matis BR, Baldwin JW, Macaveiu L, Murray JS, Politzer P (2012) J Phys Chem A 116:8644–8652
82. Kulshrestha P, Sukumar N, Murray JS, Giese RF, Wood TD (2009) J Phys Chem A 113:756–766